Express Polymer Letters Vol.16, No.6 (2022) 591–606
Available online at www.expresspolymlett.com
https://doi.org/10.3144/expresspolymlett.2022.44

Research article

Measurement of the elastic properties of epoxy resin/polyvinyl alcohol nanocomposites by ultrasonic wave velocities

Imran Oral[1*], *Mürsel Ekrem*[2]

[1]Department of Physics Education, Necmettin Erbakan University, 42090 Konya, Turkey
[2]Department of Mechanical Engineering, Necmettin Erbakan University, 42090 Konya, Turkey

Received 13 November 2021; accepted in revised form 14 February 2022

Abstract. The polyvinyl alcohol (PVA) nanofiber mats are produced using the electrospinning method. The epoxy resin (ER)/polyvinyl alcohol (PVA) nanocomposites are obtained by adding PVA nanofiber mats into neat epoxy resin (ER) as 5, 10, and 15 layers. The elastic properties (elastic constants, Young's modulus, Poisson's ratio, and Shear modulus) of the neat ER, and the ER/PVA nanocomposites, are determined by ultrasonic longitudinal wave velocity (V_L) and shear wave velocity (V_S) measurements. The morphology of the neat ER and the ER/PVA nanocomposites is investigated using scanning electron microscopy (SEM). The results obtained from SEM images showed the ER/PVA nanocomposites have a transversely isotropic structure. The V_L value of isotropic neat ER was obtained higher than the value of V_{L33} and $V_{L45°}$ but lower in $x(1)$ direction for V_{L11} in the ER/PVA nanocomposites. The velocity values of ultrasonic shear waves propagated in $x(1)$ direction and polarized in $y(2)$ direction in the ER/PVA nanocomposites are determined as higher than the velocity values of ultrasonic shear waves propagated in $z(3)$ and polarized in $x(1)$ direction. Also, the value of E_3 determined in the $z(3)$ direction is found to be significantly higher than the value of E_1 determined in the $x(1)$ direction when the number of PVA layers increased in the ER matrix. The value of shear modulus (G_{31}) is found as 1.53, 1.76, and 1.61 GPa for the ER/PVA-5, the ER/PVA-10, and the ER/PVA-15, respectively. The Poisson's ratio values of the ER/PVA nanocomposites are determined as between 0.473–0.502 and 0.247–0.276 for μ_{11} and μ_{31}, respectively. On the other hand, the degree of anisotropy in the ER/PVA nanocomposites is determined using ratios of E_1/E_3 and μ_{11}/μ_{31}. A small degree of anisotropy in dynamic Young's modulus (0.93–0.99) is observed, while a higher ratio is observed for Poisson's ratio (1.71–2.03) with increasing PVA layers in neat ER.

Keywords: *mechanical properties, ultrasound, elastic properties, electrospinning, polyvinyl alcohol*

1. Introduction

Epoxy resin (ER) is a very popular matrix used in forming composite materials as a thermoset polymer. However, it exhibits brittle fracture behavior. Therefore, most of the research about ER, and ER composites are carried out to improve their durability against external forces [1–6]. The contribution of micro, nanoorganic, or inorganic particles into pure ER is one of the most famous processes for improving the elastic properties of the ER. Many pieces of research carried out investigating the effect of reinforcing fillers in polymer matrices have proved the increased mechanical, electrical, physical, and thermal properties of these matrices [7–11]. Therefore, recently, most composite materials have been produced by adding different fillers such as glass, silica, and carbon fibers into polymer matrices to eliminate the deficiencies in their physical properties. For example, Ragosta *et al.* [8] found that adding silica particles that have 10–15 nm formed a twofold increase in fracture toughness of mechanical properties of epoxy resin. It was figured out that adding silica nanoparticles into an

*Corresponding author, e-mail: oralimran@erbakan.edu.tr

epoxy resin matrix as an amount of 3 wt% increases the tensile strength by 115% [11]. However, the most appropriate compound ratio and filler should be used to obtain composites that have good physical properties. Recently, adding nanofibers and nanoparticles into matrices such as epoxy resin has been introduced as a very effective way to produce composites' enhanced physical properties.

Nanofibers can be synthesized through different methods (drawing, phase separation, template synthesis, self-assembly, and electrospinning) [12]. Electrospinning is a simple and effective manufacturing technique used to create ultra-fine fibers from a wide variety of materials such as polymers, composites, and ceramics. This technique is based on the principle of positioning the electrically charged liquid polymer in the form of a continuous fiber on a grounded surface. The electrospinning method includes the application of the Coulomb force that exists from an electric charge, which elongates the polymer solution by electric charge exposure [12]. Electrospinning has been rapidly become a well-known method to obtain nanofibers because ultrafine fibers ranging from 50 to 500 nm in diameter can be produced by the electrospinning method. The considerable characteristics of electrospinning fiber mats are low density, large surface, very tight pore size, high pore volume, and wet absorption, which help fast and efficient adsorption [12, 13]. Therefore, different kinds of nanofibers such as poly (vinyl alcohol) (PVA), poly(urethane), chitosan (CS), poly(ethylene oxide) (PEO), poly(ethylene terephthalate) (PET), polycaprolactone (PCL), poly(lactic acid) (PLA), nylon-6 cellulose acetate using electrospinning method have been synthesized. PVA has many good characteristics, such as water-soluble, non-toxic, biocompatible, and highly hydrophilic [14]. However, the mechanical properties such as inefficient durability against external forces and low mechanical resistance are weak. Therefore, PVA has been used with matrix systems to solve these problems [12, 13, 15]. Also, PVA has been used in many polymer nanocomposites [16–22]. Tamulevičius *et al*. [23] stated that adding cupric nanoparticles to PVA improved the tensile strength and Young's modulus of the nanocomposite compared to neat PVA. Also, Zahid *et al*. [22] figured out that inserting PVA nanofibers with carbon nanoparticles gives higher mechanical, thermal, and optical properties compared to neat PVA, as well.

However, determining elastic properties by the destructive method can be sufficient for many isotropic materials. However, determining all elastic constants of anisotropic materials is so complex and sometimes impossible [24]. Thus, calculations of elastic properties by DT methods is so difficult, time-consuming, and not economical as well. The acoustic mismatch between solid, liquid, and gas mediums allows us to use Ultrasonic Testing (UT) methods. The microstructure of materials sensitively affects the ultrasonic wave velocities, acoustic impedance, and attenuation coefficient of materials. Therefore, all the elastic constants of materials can be determined using the velocity values of longitudinal and shear waves, which propagate in the appropriate directions of the materials [24]. Unlike DT methods, the determination of elastic properties in materials is much easier with UT methods. Also, UT gives higher repeatability and accuracy as well as DT methods [25]. UT is one of the most capable nondestructive testing (NDT) methods used in the characterization and quality control of composites [25–28]. UT has been conducted for determining the elastic properties of different materials [7, 29–31] and in the characterization of internal damages, defects, and discontinuities in isotropic materials [32–35].

On the other hand, it was shown that UT methods could be used for the determination of elastic constants of anisotropic materials [24, 36–39] such as carbon fibers [40], rocks [41], wood [42], and bones [43]. For instance, Mistou and Karama [37] were calculated the elastic constants of glass fiber reinforced glass/polyester composites using both DT and UT methods. The results of DT and UT methods were compared with each other. It was figured out that UT can be conducted precisely to determine the elastic properties of the glass/polyester composites. Güzel *et al*. [36] were determined the elastic constants of orthotropic E-glass/epoxy and carbon/epoxy composites using UT. The effect of E-glass and carbon fibers oriented in different directions on the elastic properties of anisotropic E-glass/epoxy and carbon/epoxy composites using UT. In another research carried out by Wong *et al*. [24], the elastic constants of transversely isotropic sedimentary shales were determined by both UT and DT methods. It was figured out that the elastic constants values of sedimentary shales determined with the DT method were much lower than those determined with the UT method.

Recently, although there are attempts to determine the elastic properties of anisotropic materials using UT [24, 36, 37, 39, 40, 42], experimental determination of elastic constants using UT methods, especially in anisotropic nanocomposites, remains challenging. However, as far as we know, no research determined the elastic properties of the transversely isotropic ER/PVA nanocomposites using the UT methods has been carried out in the literature so far. Thus, this research is carried out to determine the effect of the number of PVA layers on the transversely isotropic ER/PVA nanocomposites' elastic properties and determine the most appropriate combination ratio between ER and PVA layers using the ultrasonic wave velocity measurement method.

2. Materials and methods

2.1. Materials

In this research, the epoxy resin MGS-LR160 (Hexion, Ohio, USA) the hardener MGS- LH160 (Hexion, Ohio, USA) are used as a thermosetting matrix and as a curing agent, respectively. Polyvinyl alcohol (PVA) (Merck, Darmstadt, Germany) is used for obtaining nanofibers. Also, sodium dodecyl sulfate (SDS) (Merck, Darmstadt, Germany) is used as a general anionic surfactant. For separating PVA nanofibers from the mold, a release agent called Polivaks (Poliya Corp., Istanbul, Turkey) is used, as well. The detailed information about chemical materials is given in Table 1.

2.2. Preparation of PVA nanofiber mats and ER/PVA nanocomposites

The PVA nanofibers are produced using the electrospinning method. The production process is given step by step in Table 2.

The PVA nanofibers produced in the form of sheets over aluminum foil with dimensions of 280 mm × 300 mm by electrospinning method are cut into the size of 8 mm × 125 mm. Then, these PVA nanofiber mats are separated from aluminum foil. A chrome-nickel mold consists of 3 parts, including a filled substrate of 5 mm × 135 mm × 165 mm and 2 molds of 0.4 mm × 125 mm × 155 mm dimensions, the middle of which is kept empty according to ASTM standards is used for nanocomposite production. To

Table 1. Detailed information about chemical materials used in the research.

Variables		Epoxy resin MGS-LR160	Hardener MGS-LH160	PVA	SDS
Density at 25 °C	[g/cm^3]	1.13–1.17	0.96–1.00	1.19–1.31	1.1
Viscosity	[mPa·s]	700–900	10–50	–	–
Melting point	[°C]	–	–	230	206
Molecular weight	[g/mol]	–	–	124 000	288.38

Table 2. The production process of PVA nanofiber mats.

Step №	Step	Step explanation
1	Preparing the PVA solution	10 wt% PVA was added to 90 wt% pure water and heated to 80 °C.
2	Magnetic stirring	The PVA solution obtained in step 1 was mixed with a magnetic stirrer for 3 h at 400 rpm.
3	Preparing the SDS solution	1 wt% of SDS and 99 wt% of pure water were mixed at 25 °C.
4	Magnetic stirring	The SDS solution obtained in step 3 was mixed with a magnetic stirrer for 10 min at 400 rpm.
5	Mixing the PVA solution with the SDS solution	To reduce surface tension, 9 g of the PVA solution obtained at step 2 and 1 g of the SDS solution obtained at step 4 were mixed.
6	Magnetic stirring	The PVA+SDS mixture obtained at step 5 was mixed with a magnetic stirrer for 30 minutes at 400 rpm.
7	Loading mixture to a syringe capillary tube	About 4 ml of the mixture obtained at step 6 was loaded into a syringe-capillary tube with an orifice diameter of 0.8 mm.
8	Electrospinning	The gap between the spinneret and rotating collector was fixed at 120 mm. The feeding rate of 1.3 ml/h was applied while the collector was rotating at a constant velocity of 5 mm/s. The electrospinning process was carried out by applying 25 kV between the spinneret and rotating collector at room temperature.
9	Obtaining the PVA nanofiber mats	The PVA nanofiber mats removed from the rotating drum were dried at 60 °C under vacuum for 1 h. The PVA nanofiber mats were obtained.

prevent the epoxy resin from sticking and to separate the upper and lower molds easily, Polivaks is applied to the molds as a mold release agent. Then, a non-stick polytetrafluoroethylene film with a size of 155 mm × 125 mm and a thickness of 13 μm has adhered between the lower and upper molds, having 0.4 mm thickness. After that, for producing the ER/PVA nanocomposites, first, the PVA nanofibers with a size of 8 mm × 125 mm were placed into the mold as 5 layers. The curing agent added epoxy resin is syringed carefully onto the nanofiber in the mold until all fibers are wetted. To remove the air bubbles from the samples, all samples are kept in the vacuum environment gradually at 0.6, 0.3, and 0.2 bar for 10 min. It is then kept under a vacuum of 0.2 bar for 24 h at room temperature for pre-curing. Then, the final curing process is completed at 80 °C for 15 h. As a result, ER/PVA-5 nanocomposite is obtained. ER/PVA-10 and ER/PVA-15 samples are produced by the same process carried out for the ER/PVA-5 nanocomposite sample. For ER/PVA-10 production, PVA nanofibers with a size of 8 mm × 125 mm are placed into the mold as 10 layers while 15 layers for ER/PVA-15 nanocomposite. The thickness of all samples was determined as 1.30 mm. The abbreviations of the obtained materials are given in Table 3.

2.3. Measurements

2.3.1. Morphological measurements

Scanning electron microscopy (SEM) is used to figure out the interface between PVA nanofibers and ER matrix. SEM images of ER and ER/PVA nanocomposites are obtained using Hitachi-SU 1510 (Hitachi, Tokyo, Japan) at 20 kV voltage.

2.3.2. Density, thickness, and ultrasonic wave velocity measurements

Density measurements

The densities of the materials are determined by Archimedes' principle-based measurement system. The density measurements are carried out by an analytical balance, which has 220 g capacity and 0.1 mg readability (Radwag AS220/C/2, Radom, Poland) and a kit of density (Radwag 220, Radom, Poland). In the first step of density measurement, the temperature of the water is introduced to the Radwag AS220 balance; in the second step, the mass of the samples is measured in air, and in the third step, the mass of each sample is measured in water as well. Finally, the density of each sample is automatically determined by a semi-analytical balance. The average percentage error is determined as 0.6% for the density measurements in this research.

Table 3. Abbreviations of obtained materials in the research.

Samples' abbreviation	Number of PVA layers
ER	0
ER/PVA-5	5
ER/PVA-10	10
ER/PVA-15	15

Thickness measurements

The thickness of each sample is measured by an analog micrometer (Somet, Bilina, Czechia). Density measurements and all the other ultrasonic wave velocity measurements are repeated ten times for each sample. The average of ten measurements is recorded as the thickness of a sample. This process is repeated for each sample. Thus, all densities of all materials are determined.

Ultrasonic wave velocity measurements

There are many techniques to use in ultrasonic waves velocity measurements such as pulse-echo, peak detection, the pulse-echo overlap method (PEOM), cross-correlation, phase measurement methods [44, 45], and the through-transmission. The ultrasonic wave veloc
ity in materials can be measured highly accurately by the PEOM [44]. Therefore, the ultrasonic wave velocities are measured by the PEOM at room temperature (Figure 1).

The ultrasonic wave velocity measurements are carried out with a flaw detector (Epoch-XT-Panametrics Olympus, Massachusetts, USA), a 10 MHz longitudinal wave contact transducer (V127-Panametrics Olympus, Massachusetts, USA), and a 5 MHz shear wave contact transducer (V155-Panametrics Olympus, Massachusetts, USA), as well. The coupling medium has a considerable influence on ultrasonic

Figure 1. Measurement set-up system and tools used for ultrasonic wave velocities.

wave velocity [46]. Therefore, the longitudinal wave velocity measurements are conducted using glycerin (BQ Panametrics Olympus, Massachusetts, USA), while ultrasonic shear wave velocity measurements are carried out using shear wave coupling (SWC Panametrics Olympus, Massachusetts, USA).

The ultrasonic longitudinal and shear waves' velocity measurement process is carried out in the PEOM as follows: Only one transducer is used to transmit and receive the ultrasonic wave signals in the PEOM. For highly accurate measurement, polymethylmethacrylate (PMMA) sample is used as reference material in this research. Glycerin is applied to this PMMA reference sample. The whole received pulse-echo train is displayed on the screen of the Epoch-XT flaw detector. Then, the first back wall echo is selected. The time of flight of the first back wall echo (t_1) for the reference sample is figured out. After applying coupling on the upper face of the PMMA sample, a sample is put over the PMMA reference sample, and coupling is applied again before putting the transducer over the upper face of the test sample. Data of the first back wall echo for reference + composite samples (t_2) is determined. The time of flight between two measurements (Δt) is determined by overlapping the first back wall echos of two measurements. These data obtained for reference and reference+sample is transferred to the computer using a USB flash disk. The time of flight between two measurements (Δt) is calculated using Microsoft-Excel Software, as shown in Figure 2.

After defining the time of flight between these back wall echos, the velocity of ultrasonic waves propagating through the test sample is determined by Equation (1):

$$V = \frac{2d}{\Delta t} \tag{1}$$

where V, d, and Δt are the ultrasonic wave velocity, the thickness of the sample, and the time-of-flight between subsequent back wall signals on the screen of the flaw detector, respectively. Each measurement is repeated ten times to improve the accuracy of measurements. The percentage error for both the ultrasonic longitudinal wave velocity and shear wave velocity measurements was about 1%.

2.3.3. Determination of elastic properties of transversely isotropic nanocomposites

Because of the morphological analysis, it is figured out that the nanocomposite materials' structure is approximately transversely isotropic. The elastic constants (c_{ij}) of transversely isotropic materials are related to the bulk density, the direction of the axis of symmetry, and the velocities of ultrasonic waves [39, 47, 48]. Therefore, the elastic constants of transversely isotropic materials can be calculated using ultrasonic longitudinal and shear waves, which propagate in the appropriate directions of the material, and bulk density. These materials have five independent elastic constants (c_{11}, c_{33}, c_{44}, c_{66}, and c_{13}). The sample's scheme can be used for ultrasonic velocity measurements, which are given in Figure 3.

Shear wave velocity values (V_{sij}) and longitudinal wave velocity values (V_{Lii}) in x, y, and z directions should be measured for the determination of elastic

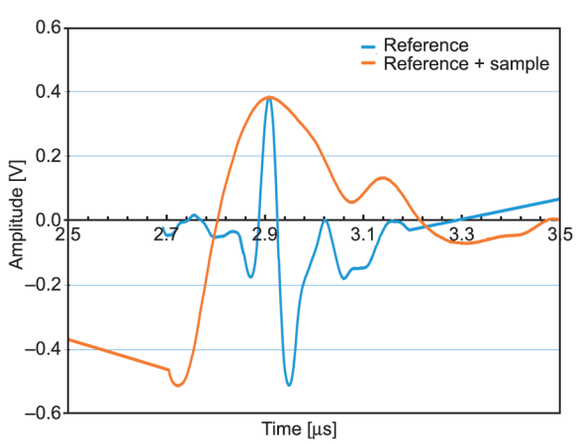

Figure 2. A snapshot showing the overlapping of the signals in PEOM.

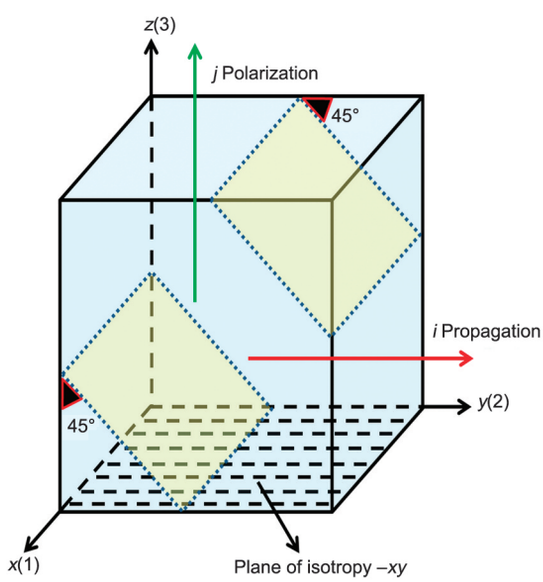

Figure 3. Sample's scheme for the measurement of ultrasonic wave velocities in transversely isotropic materials.

constants in the UT method. Also, the tested sample should be cut to the angle of 450 with x and y-axes to measure the longitudinal wave velocity, abbreviated as $V_{L45°}$. However, since the thickness of the ER/PVA nanocomposites obtained was not sufficient, it was impossible to cut the samples at an angle of 45° as given in Figure 3. For this reason, the approximate values of $V_{L45°}$ in the nanocomposite materials produced in this research were calculated from the velocity ratio. Because the velocity ratio generally depends on many factors such as differential pressure, porosity, pore geometry, and degree of consolidation, it has been used in many applications such as determining the degree of consolidation, estimating the velocities, and defining the pore fluid [49]. For example, the longitudinal wave velocity (V_L)/shear wave velocity (V_S) ratios were found as 1.9 and 1.8 for limestone and sandstone, respectively [50]. The velocity ratio of $V_{L45°}$ to V_{L11} measured in some transversely isotropic materials in the literature is approximately equal to the value of 0.94 [24]. Therefore, the value of $V_{L45°}$ in transversely isotropic ER/PVA nanocomposites is calculated using the experimentally measured V_{L11} value and 0.94 value, as well. More detailed literature about velocity ratio application to predict ultrasonic velocities can be seen in the research carried out by Lee [49].

The vibration direction of the particles in the material and the direction of propagation of the ultrasonic waves used in the calculation of elastic constants in transversely isotropic materials are given in Table 4. The relations between the transversely isotropic materials' density (ρ), elastic constants, and ultrasonic wave velocities are defined as given in Equation (2) below [24]:

$$\begin{aligned} c_{11} &= \rho \cdot V_{L11}^2 \\ c_{33} &= \rho \cdot V_{L33}^2 \\ c_{44} &= \rho \cdot V_{S31}^2 \\ c_{66} &= \rho \cdot V_{S12}^2 \\ c_{13} &= \rho \cdot \left(2 \cdot V_{L45°}^2 - V_{L11}^2 - 2 \cdot V_{S31}^2\right) \end{aligned} \tag{2}$$

Young's modulus (E_1 and E_3), Poisson ratios (μ_{11} and μ_{31}) and shear modulus (G_{31}) of the ER/PVA nanocomposites used in this research are determined using Equation (3)–(5) [24]:

$$\begin{aligned} E_1 &= \frac{4c_{66}\left(c_{11}c_{33} - c_{13}^2 - c_{33}c_{66}\right)}{c_{11}c_{33} - c_{13}^2} \\ E_3 &= \frac{c_{11}c_{33} - c_{13}^2 - c_{33}c_{66}}{c_{11} - c_{66}} \end{aligned} \tag{3}$$

$$\begin{aligned} \mu_{11} &= \frac{c_{11}c_{33} - c_{13}^2 - 2c_{33}c_{66}}{c_{11}c_{33} - c_{13}^2} \\ \mu_{31} &= \frac{c_{13}}{2\left(c_{13} - c_{66}\right)} \end{aligned} \tag{4}$$

$$G_{31} = c_{44} \tag{5}$$

The percentage error is determined as ±2.30 and ±7.34% for elastic constants measurements and elastic modulus measurements, respectively.

2.3.4. Determination of elastic properties of neat ER

The mathematical relationship between elastic constants and ultrasonic waves' velocity is defined for isotropic materials [51]. Because that hardened neat ER is an isotropic material, the elastic properties of neat ER are determined using Equation (6)–(10) [52, 53].

$$L = \rho V_L^2 \tag{6}$$

$$G = \rho V_S^2 \tag{7}$$

$$E = 2G(1 + \mu) \tag{8}$$

$$\lambda = \rho\left(V_L^2 - 2V_S^2\right) \tag{9}$$

$$\mu = \frac{L - 2G}{2(L - G)} \tag{10}$$

Table 4. Ultrasonic wave velocities propagated in transversely isotropic materials, and their propagation directions.

Ultrasonic wave velocity [m/s]	Wave type and propagation direction	Vibration direction of particles
V_{L11}	Longitudinal wave propagating along x-axis.	x-axis
V_{L33}	Longitudinal wave propagating along z-axis	z-axis
V_{S31}	Shear wave propagating along z-axis	x-axis
V_{S12}	Shear wave propagating along x-axis	y-axis
$V_{L45°}$	Longitudinal wave propagating along 45°	45° to x-y axis

where V_L, V_S, L, G, E, λ, μ, and ρ are the longitudinal wave velocity, shear wave velocity, Longitudinal modulus, Shear modulus (or Lame's second constant), Young's modulus, Lame's first constant, Poisson's ratio, and density of the samples, respectively. The physical properties of isotropic materials are independent of direction. Therefore, if longitudinal wave velocities abbreviated as V_{L11}, $V_{L45°}$, and V_{L33} are equal in the isotropic neat ER then V_L given in Equation (6), (8)–(10) will be equivalent to values of V_{L11}, $V_{L45°}$, and V_{L33} given in Equation (2), as well. Similarly, if the shear wave velocities abbreviated as V_{S12} and V_{S31} are equal in the ER, V_S given in Equation (7)–(10) will be equivalent to V_{S12} and V_{S31}, as well. In this case, longitudinal modulus (L) of ER given in Equation (6) will be equivalent to the elastic constant of $c11$ (or $c33$). Shear modulus (G) of ER will be equivalent to the elastic constant of c_{44} (or c_{66}), and Lame's constant (λ) will be equivalent to the elastic constant of c_{13} given in Equation (2). Thus, the relation between variables will be as $V_L = V_{L11} = V_{L45°} = V_{L33}$, $V_S = V_{S12} = V_{S31}$, $L = c_{11} = c_{33}$, $G = c_{44} = c_{66}$, and $\lambda = c_{13}$. Also, the elastic modulus given in Equation (3) will give the elastic modulus values given in Equation (8) for isotropic neat ER such as $E = E_1 = E_3$, $\mu = \mu_{11} = \mu_{31}$, and $G = G_{31}$.

3. Results and discussions

In this research, the ER/PVA nanocomposites have different PVA fiber mats (5, 10, and 15) are produced and their elastic properties are determined using the UT method. Morphology of the neat ER, and ER/PVA nanocomposites are analyzed using SEM images given in Figure 2. Data related to density, ultrasonic wave velocities, elastic constants, elastic moduli, Poisson's ratio, and degree of anisotropy values obtained for neat ER and the ER/PVA nanocomposites are given in Tables 5–7, and Figures 4–10. These obtained results are analyzed and discussed in this part of the research.

3.1. Morphological results

SEM images of the fracture surfaces of the samples are examined. Figure 4 reveals 5000, and 10 000 magnification SEM images obtained for neat ER, PVA nanofiber mats, and ER/PVA-15 nanocomposites.

The diameter of PVA nanofibers is determined from SEM images ranging between 220 and 400 nm. It is also seen that some nanofibers have increased in diameter. The reason for this increase is that during the production of composite, nanofibers absorb some epoxy before curing. This situation clearly shows that nanofibers can be wetted effectively and homogeneously with epoxy. When the fibers are homogeneously distributed in the epoxy matrix, they increase fracture toughness between the layers by forming secondary cracks at the crack tip or by reducing the stress density at the crack tip by crack bridging. The stripping of the nanofibers from the matrix, the absorption of the epoxy by the nanofibers, and the bridging effect during breakage play an effective role in increasing the toughness of the composite materials produced.

According to the SEM images in Figures 4c and 4d, the PVA nanofibers are bead-free, homogeneous, and have a smooth surface. Generally, when the SEM images are examined, it is seen that there is a good wettability between fiber breakage, stripping of fibers from epoxy, epoxy resin wrapping around the fibers, and epoxy-fiber (Figures 4e and 4f). The interface between fillers and the polymeric matrix is essential in polymeric composites [54]. As can be seen from SEM images in Figures 4e and 4f, the PVA nanofibers were homogeneously distributed in the ER matrix. The most compatible interaction between fillers and matrices in composite materials enhances the mechanical properties. In this context, when the elastic constants and elastic modulus values are given in Table 6 and Table 7, respectively, were analyzed, it can be seen that the best interface between PVA nanofibers and ER matrix was formed for the ER/PVA-10 nanocomposite. Figures 4e and 4f also show that a random distribution of PVA nanofibers along the x-axis and y-axis has occurred in the ER matrix. This random distribution in the x-axis and y-axis explains the reason why these nanocomposites' structures were predicted as transversely isotropic.

3.2. Density and ultrasonic wave velocity results

The density, longitudinal wave velocity, and shear wave velocity values of neat ER and the ER/PVA nanocomposites are given in Table 5.

According to data of Table 5 and Figure 5, density values ranged from 1152 kg/m^3 (for neat ER) to 1193 kg/m^3 (for ER/PVA-15). The density value of ER/PVA-15 was determined as the highest density. However, it was addressed that there is a relationship between ultrasonic wave velocity and materials'

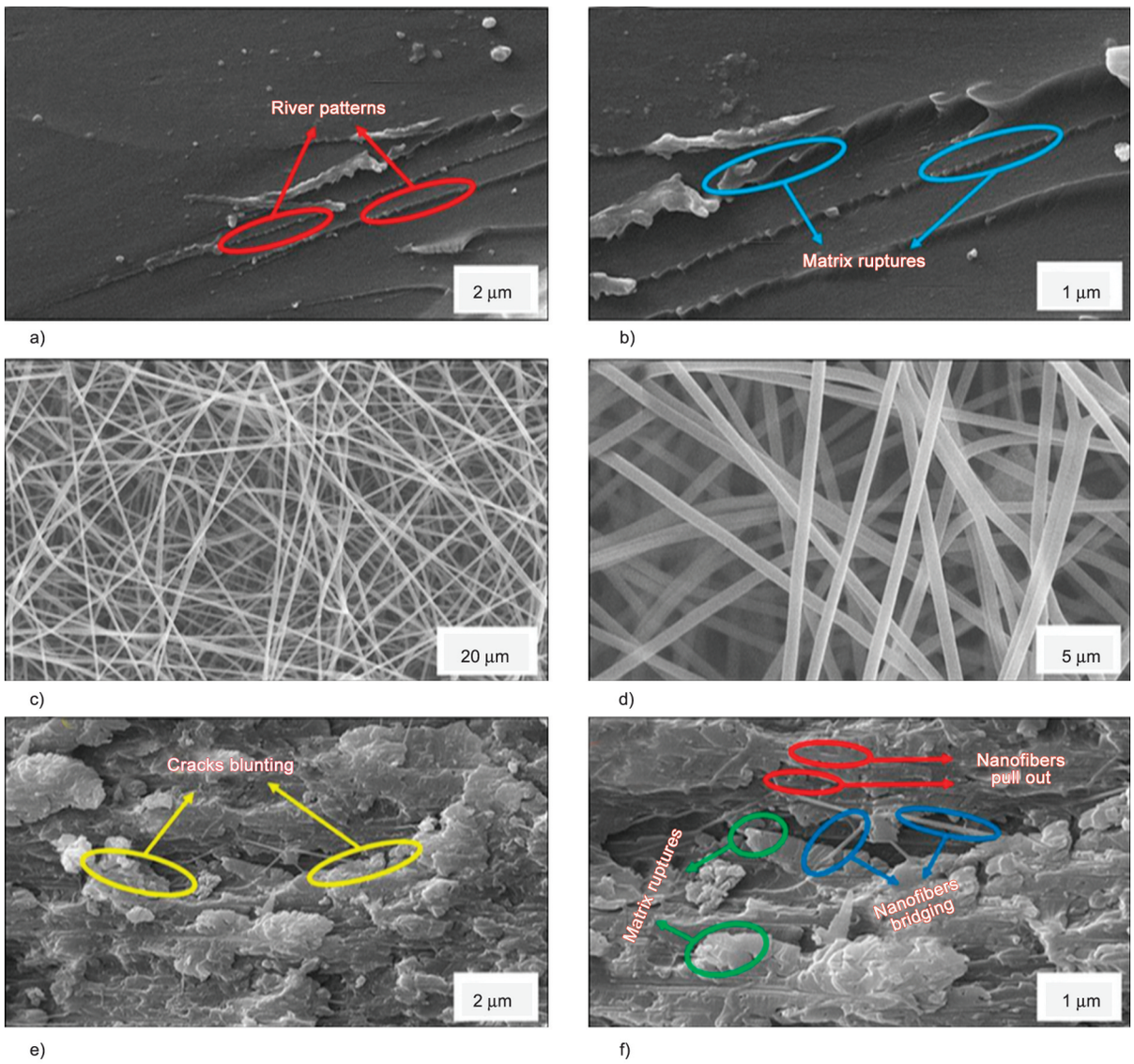

Figure 4. SEM images: a) neat ER 5000×, b) neat ER 10 000×, c) PVA nanofiber mats 5000×, d) PVA nanofiber mats 10 000×, e) ER/PVA-15 nanocomposite 5000×, f) ER/PVA-15 nanocomposite 10 000×.

density [55, 56]. It was indicated that the ultrasonic wave velocity tends to increase with an increase in the density of the sample. The results obtained about the relationship between densities and ultrasonic wave velocities of samples were sometimes in good agreement [55, 56], while sometimes were not in good agreement [57] with some results from the literature. For example, Ilic [57] figured out that ultrasonic wave velocity was not dependent on the density.

Table 5. The densities [kg/m^3] and ultrasonic wave velocities [m/s] of ER and the ER/PVA nanocomposites.

Samples	ρ [kg/m^3]	V_{L11} [m/s]	V_{L33} [m/s]	$V_{L45°}$ [m/s]	V_{S12} [m/s]	V_{S31} [m/s]
ER	1152	2690	2690	2690	1189	1189
ER/PVA-5	1153	2843	2622	2673	1283	1153
ER/PVA-10	1154	2853	2632	2684	1288	1236
ER/PVA-15	1193	2848	2627	2678	1285	1161

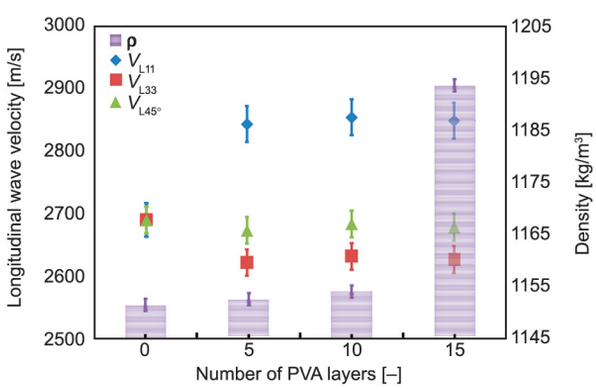

Figure 5. Variation in density and longitudinal wave velocity with number of PVA layers in neat ER and ER/PVA nanocomposites.

Also, the densities of the ER/PVA nanocomposites increases with increasing number of PVA layers compared with neat ER. This result is compatible with results that found an increase in density with increasing filler content in composites [7, 58, 59]. Solid materials' density depends on different variables like crosslink density, the dimensionality of interstitial spaces, structure, and coordination number [60]. Therefore, the variation in the density of composite materials may give important information about their elastic properties.

According to Table 5 and Figure 5, the longitudinal wave velocities have different values in different directions. This result supports data of SEM images, which indicates that the ER/PVA composites have a transversely isotropic structure. When the V_{L11}, V_{L33}, and $V_{L45°}$ values measured in different directions are compared, it is seen that they are generally ranked as $V_{L11} > V_{L45°} > V_{L33}$. It is clear that the longitudinal wave velocity value of isotropic neat ER is higher than of the ER/PVA nanocomposites for V_{L33} and $V_{L45°}$ velocities but lower in $x(1)$ direction for V_{L11}. This result indicates that adding PVA layers into the ER occurred a significant increase in the longitudinal wave velocity values in the $x(1)$ direction. When the ER/PVA nanocomposites were compared, the highest longitudinal wave velocity value (2853 m/s) was obtained when 10 PVA layers were added to the ER. Also, when the number of PVA layers added to the ER is increased from 10 to 15, it is seen that the longitudinal wave velocity decreases slightly. This result also shows that adding 10 PVA layers to pure ER is the most appropriate ratio.

The data of Table 5 and Figure 6 shows that shear wave velocity values of nanocomposites lie in ranges of 1153–1288 m/s. Also, it is seen that values of ultrasonic shear waves in the ER/PVA nanocomposites propagate in $x(1)$ direction and polarize in $y(2)$ direction are higher than the values of ultrasonic shear waves propagating in $z(3)$ and polarize in $x(1)$ direction.

The shear wave velocity values obtained are plotted in Figure 6. The velocity values of shear waves' that propagate in $x(1)$ direction and polarized in $y(2)$ direction ranged from 1283 to 1288 m/s. However, the value of shear wave velocities propagating in $z(3)$ direction and polarized in $x(1)$ direction ranged from 1153 to 1236 m/s. The shear wave velocity value of neat ER was determined as 1189 m/s. According to these findings, it can be stated that all nanocomposites' shear wave velocity values were increased in the $x(1)$ direction. The fact that the PVA nanofibers are in the epoxy resin along the $x(1)$ direction, but the PVA layers are parallel to each other in the $z(3)$ direction, and the bottom and top surfaces of these PVA layers are covered with epoxy resin, is assumed to be the reason of the higher ultrasonic shear wave velocity values in the $x(1)$ direction than of in the $z(3)$ direction. The contrary of this result, except for the value of the ER/PVA-10 nanocomposite sample, the other values were found lower than the neat ER in the $z(3)$ direction. Therefore, it can be stated that adding PVA into ER improves nanocomposites' shear wave velocity values in the $x(1)$ direction.

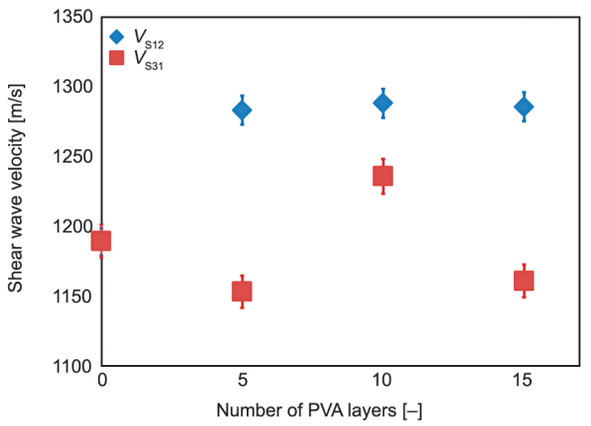

Figure 6. Variation in ultrasonic shear wave velocities with number of PVA layers in neat ER and ER/PVA nanocomposites.

3.3. Elastic constants results

The elastic constants of ER and the ER/PVA nanocomposites calculated using Equation (2) and are given in Table 6 and illustrated in Figure 7.

According to Table 6 and Figure 7 data, the highest elastic constant value of the ER/PVA nanocomposites was found for the c_{11}, while the lowest values were found for c_{44}. The values of c_{11} elastic constant, which propagate in the $x(1)$ direction and polarized in the $x(1)$ direction, ranged from 9.31 to 9.68 GPa. The values of c_{33} constant, which propagate in $z(3)$ direction and polarized in $z(3)$ direction, ranged from 7.92 to 8.24 GPa. The values of c_{44} ranged from 1.53 to 1.76 GPa. The values of c_{66} ranged from 1.90 to 1.97 GPa, while the values of $c13$ ranged from 3.70 to 4.23 GPa.

According to the obtained data given in Table 6, the ER/PVA nanocomposites' c_{11} and c_{66} values were

Table 6. The elastic constant values of ER and ER/PVA nanocomposites.

Samples	c_{11} [GPa]	c_{33} [GPa]	c_{44} [GPa]	c_{66} [GPa]	c_{13} [GPa]
ER	8.33	8.33	1.63	1.63	5.08
ER/PVA-5	9.31	7.92	1.53	1.90	4.09
ER/PVA-10	9.40	8.00	1.76	1.91	3.70
ER/PVA-15	9.68	8.24	1.61	1.97	4.23

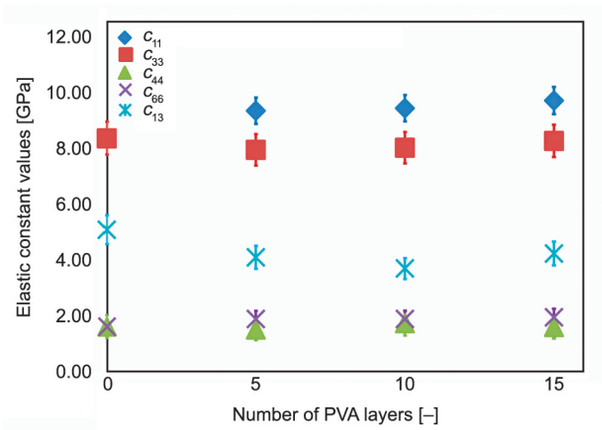

Figure 7. Variation in elastic constants with number of PVA layers in neat ER and ER/PVA nanocomposites.

Table 7. Comparison elastic modulus values of ER and ER/PVA nanocomposites.

Samples	E_1 [GPa]	E_3 [GPa]	G_{31} [GPa]	μ_{11} [–]	μ_{31} [–]	E_1/E_3 [–]	μ_{11}/μ_{31} [–]
ER	4.49	4.49	1.63	0.378	0.378	1	1
ER/PVA-5	5.59	5.66	1.53	0.473	0.276	0.99	1.71
ER/PVA-10	5.75	6.17	1.76	0.502	0.247	0.93	2.03
ER/PVA-15	5.82	5.92	1.61	0.475	0.274	0.98	1.73

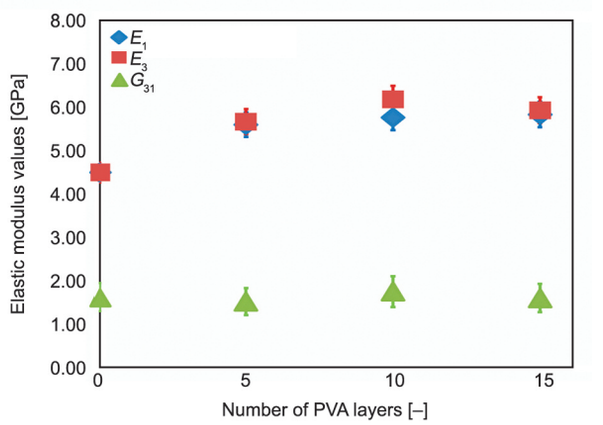

Figure 8. Variation in elastic modulus values with number of PVA layers in neat ER and ER/PVA nanocomposites.

found as higher than the values of neat ER. Also, it can be stated that the values of c_{33} and c_{13} constants of neat ER were found as higher than the values of the ER/PVA nanocomposites. However, except for the c_{44} value of ER/PVA-10 sample, the c_{44} value of neat ER was found as higher than other ER/PVA nanocomposites as well. These results prove that the values of elastic constants are very sensitive to variation in measured ultrasonic wave velocities [24]. The variation behavior of elastic constants in the ER/PVA nanocomposites was found as similar to the behavior of ultrasonic wave velocity in nanocomposites.

3.4. Elastic modulus and Poisson's ratio results

The measured elastic modulus and Poisson's ratio values of obtained nanocomposites and ER were determined using Equations (3)–(5). The data obtained for the value of elastic modulus and Poisson's ratio is given in Table 7 and Figures 8–10. The data given in Table 7 shows that the value of E_1 for the ER/PVA nanocomposites was determined as 5.59, 5.75, and 5.82 GPa for the ER/PVA-5, ER/PVA-10, and ER/PVA-15 nanocomposite samples, respectively.

Therefore, the value of E_1 had increased with the increasing PVA layers in the $x(1)$ direction. Also, the value of E_3 derived from the ultrasonic wave velocity measurements for the ER/PVA nanocomposites was determined as 5.66, 6.17, and 5.92 GPa for the ER/PVA-5, ER/PVA-10, and ER/PVA-15 nanocomposite samples, respectively. These results clearly figured out that increasing the number of PVA layers in ER matrix increased the value of E_3 much more than the value of E_1. The Young's modulus value of the neat PVA nanofiber mat was determined as 0.108 GPa by mechanical testing method [61]. This value of Young's modulus (0.108 GPa) is much lower than that of neat ER (4.49 GPa). The elastic coefficients of composites are generally among the elastic coefficient values of the matrix and filling materials formed the composite. Therefore, it can be stated that the ER/PVA nanocomposites obtained from the unification of PVA and ER have higher elastic constant values compared to both filler and matrix used.

Considering the value of Young's modulus of neat ER (4.49 GPa) and the variation behavior of Young's modulus seen in Figure 8, the addition of PVA layers into ER increased the E_1 and E_3 of the ER/PVA nanocomposites. However, the increase of E_3 in the $z(3)$ direction is significantly higher than the increase in E_1 in the $x(1)$ direction. These results revealed that the bonds that occurred between PVA layers and epoxy resin in the $z(3)$ direction are stronger than those in the $x(1)$ and $y(2)$ directions. Another remarkable result seen in Table 7 is that both E_1 and E_3 values of the

ER/PVA-10 nanocomposite are higher than the E_1 and E_3 values of other nanocomposites and pure ER. As can be seen from Table 7 and Figure 8, the shear modulus of the neat ER is determined to be 1.63 GPa. The value of shear modulus (G_{31}) was found as 1.53, 1.76, and 1.61 GPa for the ER/PVA-5, the ER/PVA-10, and the ER/PVA-15, respectively. Thus, the highest value of G_{31} was obtained for the ER/PVA-10 nanocomposite sample, while the lowest value was determined for the ER/PVA-5 sample. This result agrees well with values obtained for E_3 values. Based on the findings of Table 7 and Figure 8, adding especially 10 PVA layers into neat ER had formed the ER/PVA nanocomposite, which has better G_{31} and E_3 values compared to neat ER. Because adding 10 PVA layers into neat ER increased its G_{31} by about 8% while increasing its E_3 value by about 37%. Although the density of ER/PVA-15 nanocomposite is higher than that of ER/PVA-5 and ER/PVA-10 composites, its velocity and elasticity modulus values are lower than these composites. It is thought that the reason for this is that when 15 layers of PVA are placed on top of each other, the penetration of the epoxy into the PVA layers and its wettability becomes difficult. It is estimated that this situation causes the formation of air bubbles in the nanofiber materials in the ER/PVA-15 composite, decreasing in ultrasonic velocity values and elastic modulus.

Although the results obtained for E and G values in this research show similarities with the research results conducted by Yıldırım *et al*. [21], however, the results of this research are more consistent with the literature compared to the research of Yıldırım *et al*. [21]. Because the values of E_1 and E_3 determined in this research are in the range of 4–6 GPa, while the values of E are determined in the study carried out by Yıldırım *et al*. [21] are in the range of 1.62–1.70 GPa. This difference could be due to the measurement methods. Because although the ER/PVA nanocomposites are transversely isotropic, E and G values were determined using tensile tests performed in only a single direction in the research carried out by Yıldırım *et al*. [21]. But in this research, since the ER/PVA nanocomposites are transversely isotropic, E_1, E_3, and G_{31} values were determined precisely using ultrasonic velocity measurements in different directions. This result also confirms that the ultrasonic method can be used safely in such materials. Modulus of elasticity is defined as the mathematical description of a material's tendency to be deformed elastically when a force is applied to it. The elasticity constants, density, and ultrasonic waves' velocity are related to interatomic forces, fracture, porosity, crystal growth, and microstructural factors. Therefore, minor changes in elastic modulus, density, or ultrasonic velocities of many materials are very sensitive to any minor compositional changes. In this consideration, analyzing such variations using ultrasonic methods is important in material characterization.

The Poisson's ratios of all samples used in this research were calculated using Equation (4) and Equation (10). The variation for the Poisson's ratios (μ_{11} and μ_{31}) as a function of increasing PVA nanofiber layers are plotted in Figure 9. According to Table 7 and Figure 9, the Poisson's ratio of neat ER was determined as 0.378, and the Poisson's ratio values of the ER/PVA nanocomposites were determined as between 0.473 to 0.502, 0.247 to 0.276 for μ_{11} and μ_{31}, respectively. Also, it is seen that the μ_{31} values of the ER/PVA nanocomposites were lower than of both μ_{11} values of the ER/PVA nanocomposites and μ value of neat ER, as well. The lateral contraction per unit breadth divided by the longitudinal extension per unit length in simple tension was defined as Poisson's ratio [62–64]. According to Gercek [63], Poisson's ratio provides critical information related to bonding forces compared to other elastic coefficients. In this context, it can be stated that the lower values obtained for Poisson's ratio indicate an increase in the number of shear chemical bonds per atom in the network. In conclusion, it can be stated that if the crosslink density increase in a material, the Poisson's ratio value will decrease for that material as well. This conclusion agrees well with many studies from related literature [63, 65]. According to Gercek [63], the Poisson's ratio value is low for many

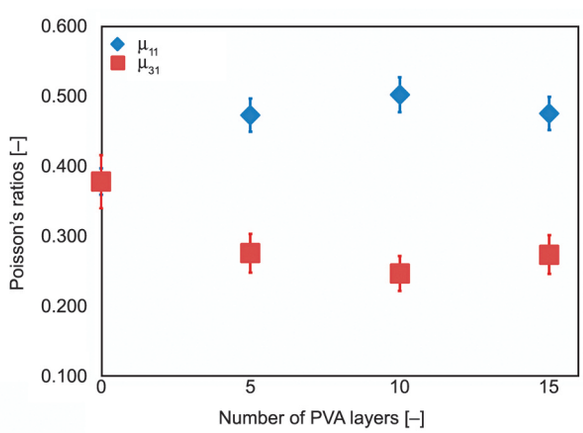

Figure 9. Variation in Poisson's ratios with number of PVA layers in neat ER and ER/PVA nanocomposites.

materials that have a high value of Young's modulus and shear modulus. Thus, it can be concluded that the lower Poisson's ratio shows an increase in the durability of materials against external forces [7]. However, this behavior of Poisson's ratio is invalid for auxetic materials that have a negative value for Poisson's ratio.

However, the lowest value of Poisson's ratio (μ_{31}) was obtained for ER/PVA-10 nanocomposite sample. The results of this research obtained for Poisson's ratio are not in good agreement with research carried out with the same materials using destructive testing methods [21]. They have found that all values of Poisson's ratio of ER/PVA nanocomposites were higher than of neat ER. It can be stated that the Poisson's ratio values measured in this research agree well with the results of related literature [56, 62, 63, 66]. Therefore, the results of this research prove the ultrasonic measurement accuracy again.

The anisotropic behavior can be determined using anisotropy ratios [24]. The degree of anisotropy in the ER/PVA nanocomposites was determined using ratios of the E_1/E_3 and μ_{11}/μ_{31}. The data of anisotropy in the ER/PVA nanocomposites was given in Table 7. The variation in the degree of anisotropy with number of PVA layers in the ER/PVA nanocomposites is plotted in Figure 10.

A small degree of anisotropy in dynamic Young's modulus was observed, while a higher was observed for Poisson's ratio with increasing PVA layers in neat ER. The degree of anisotropy measured using ratios of the E_1/E_3 in Young's modulus was ranged from 0.93 to 0.99. But, a bigger degree of anisotropy was measured using ratios of the μ_{11}/μ_{31} in Poisson's ratios were ranging from 1.71 to 2.03. The ratios of E_1/E_3 and μ_{11}/μ_{31} are independent. Therefore, they do not necessarily have to be the same [67]. These results of anisotropy obtained showed that the anisotropic structure of the ER/PVA nanocomposites can be determined by the ultrasonic method.

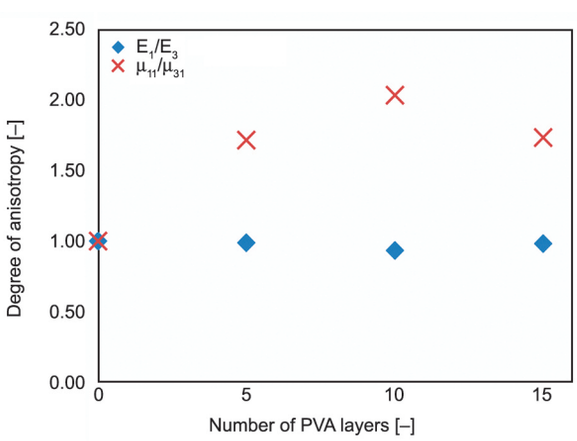

Figure 10. Variation in the degree of anisotropy with PVA layer numbers in neat ER and ER/PVA nanocomposites.

The anisotropic behavior of different materials such as London clay [68], sedimentary shale [24], and Gault clay [69] have been investigated. The degree of anisotropy for London clay was determined as 1.50 using the ratio of shear modulus values (G_{11}/G_{31}) by Jovičić and Coop [68]. Similarly, Wong *et al.* [24] have determined the degree of anisotropy of sedimentary shales using ultrasonic and static tests. They have found the degree of anisotropy using the ratio of E_1/E_3 as 1.70 and 1.10 for static test and ultrasonic wave measurement method, respectively. When they used the ratio of shear modulus values (G_{11}/G_{31}), they have found the degree of anisotropy as 1.33 and 1.24 for static and ultrasonic wave velocity measurement methods, respectively. Also, Lings [69] has determined anisotropy ratio in stiff Gault clay using the bender element test. They have determined the anisotropy of stiff Gault clay as 3.96 for Young's modulus using the ratio of E_1/E_3 and 2.25 for shear modulus using the ratio of G_{11}/G_{31}. Most studies that investigated the degree of anisotropy were generally carried out using destructive testings. Thus, determining the degree of anisotropy using nondestructive testing methods such as ultrasonic wave velocity measurement remains challenging.

4. Conclusions

In this study, the PVA nanofiber mats were produced by the electrospinning method. The transversely isotropic ER/PVA nanocomposites were obtained by adding PVA nanofiber mat into neat ER as 5, 10, and 15 layers. The effect of the PVA nanofiber mats content on elastic properties (elastic constants, Poisson's ratio, and elastic moduli) of the ER/PVA nanocomposites were determined by the PEOM. The morphologies of neat ER and ER/PVA nanocomposite samples were investigated using SEM. In line with the findings obtained, the results of the research can be summarized as follows:

1) The obtained SEM images showed that the ER/PVA nanocomposites have a transversely isotropic structure.
2) The V_L value of isotropic neat ER was obtained higher than the value of V_{L33} and $V_{L45°}$ but lower

in $x(1)$ direction for V_{L11} in the ER/PVA nanocomposites.

3) The velocity values of ultrasonic shear waves propagated in $x(1)$ direction and polarized in $y(2)$ direction in the ER/PVA nanocomposites were determined as higher than the velocity values of ultrasonic shear waves propagated in $z(3)$ and polarized in $x(1)$ direction.
4) The value of E_3 determined in the $z(3)$ direction was found to be significantly higher than the value of E_1 determined in the $x(1)$ direction when the number of PVA layers in ER matrix increased.
5) The highest shear modulus (G_{31}) value was found as 1.76 GPa for the ER/PVA-10 sample.
6) The Poisson's ratio values of the ER/PVA nanocomposites were determined as between 0.473 to 0.502 and 0.247 to 0.276 for μ_{11} and μ_{31}, respectively.
7) A small degree of anisotropy in dynamic Young's modulus (0.93–0.99) was observed, while a higher ratio was observed for Poisson's ratio (1.71–2.03) with increasing PVA layers in neat ER.
8) According to the obtained results adding 10 PVA layers into the ER is the most appropriate composition ratio for ER/PVA nanocomposites. Because adding 10 PVA layers into neat ER increased its G_{31} by about 8% while increasing its $E3$ value by about 37%.

These obtained results show that the elastic properties of transversely isotropic nanocomposites such as ER/PVA can be determined precisely using UT methods. It is important to determine the elastic properties of anisotropic materials with UT in a sensitive, fast and economical way. Thus, similar studies conducting UT methods can be suggested for the determination of elastic properties of anisotropic nanocomposites.

Acknowledgements

This research did not receive any specific grant from funding agencies in the public, commercial, or not-for-profit sectors.

References

[1] Guo S-Y., Zhang X., Ren J., Chen J-Z., Zhao T-J., Li T-W., Zhang L.: Preparation of TiO_2/epoxy resin composite and its effect on mechanical and bonding properties of OPC mortars. Construction and Building Materials, **272**, 121960 (2021). https://doi.org/10.1016/j.conbuildmat.2020.121960

[2] McDonnell C., Hayes S., Potluri P.: Investigation into the tensile properties of ISO-401 double-thread chain-stitched glass-fibre composites. International Journal of Lightweight Materials and Manufacture, **4**, 203–209 (2021). https://doi.org/10.1016/j.ijlmm.2020.11.001

[3] Pradhan S., Acharya S. K., Prakash V.: Mechanical, morphological, and tribological behavior of eulaliopsis binata fiber epoxy composites. Journal of Applied Polymer Science, **138**, 50077 (2021). https://doi.org/10.1002/app.50077

[4] Preghenella M., Pegoretti A., Migliaresi C.: Thermo-mechanical characterization of fumed silica-epoxy nanocomposites. Polymer, **46**, 12065–12072 (2005). https://doi.org/10.1016/j.polymer.2005.10.098

[5] Ruan S., Wei S., Gong W., Li Z., Gu J., Shen C.: Strengthening, toughening, and self-healing for carbon fiber/epoxy composites based on ppesk electrospun coaxial nanofibers. Journal of Applied Polymer Science, **138**, 50063 (2021). https://doi.org/10.1002/app.50063

[6] Uslu E., Gavgali M., Erdal M. O., Yazman Ş., Gemi L.: Determination of mechanical properties of polymer matrix composites reinforced with electrospinning N66, PAN, PVA and PVC nanofibers: A comparative study. Materials Today Communications, **26**, 101939 (2021). https://doi.org/10.1016/j.mtcomm.2020.101939

[7] Oral I., Soydal U., Bentahar M.: Ultrasonic characterization of andesite waste-reinforced composites. Polymer Bulletin, **74**, 1899–1914 (2017). https://doi.org/10.1007/s00289-016-1811-3

[8] Ragosta G., Abbate M., Musto P., Scarinzi G., Mascia L.: Epoxy-silica particulate nanocomposites: Chemical interactions, reinforcement and fracture toughness. Polymer, **46**, 10506–10516 (2005). https://doi.org/10.1016/j.polymer.2005.08.028

[9] Santos J. C., Vieira L. M. G., Panzera T. H., Schiavon M. A., Christoforo A. L., Scarpa F.: Hybrid glass fibre reinforced composites with micro and poly-diallyldimethylammonium chloride (PDDA) functionalized nano silica inclusions. Materials and Design, **65**, 543–549 (2015). https://doi.org/10.1016/j.matdes.2014.09.052

[10] Wu S., Li F., Wang H., Fu L., Zhang B., Li G.: Effects of poly(vinyl alcohol) (PVA) content on preparation of novel thiol-functionalized mesoporous PVA/SiO_2 composite nanofiber membranes and their application for adsorption of heavy metal ions from aqueous solution. Polymer, **51**, 6203–6211 (2010). https://doi.org/10.1016/j.polymer.2010.10.015

[11] Zheng Y., Zheng Y., Ning R.: Effects of nanoparticles SiO_2 on the performance of nanocomposites. Materials Letters, **57**, 2940–2944 (2003). https://doi.org/10.1016/S0167-577X(02)01401-5

[12] Jauhari J., Suharli A. J., Saputra R., Nawawi Z., Sriyanti I.: Polyvinylpyrollidone/cellulose acetate (PVA/CA) fiber size prediction using scaling law model. Journal of Physics: Conference Series,**1467**, 012049 (2020). https://doi.org/10.1088/1742-6596/1467/1/012049

[13] Wang D., Cheng W., Yue Y., Xuan L., Ni X., Han G.: Electrospun cellulose nanocrystals/chitosan/polyvinyl alcohol nanofibrous films and their exploration to metal ions adsorption. Polymers, **10**, 1046 (2018). https://doi.org/10.3390/polym10101046

[14] Jia Y-T., Gong J., Gu X-H., Kim H-Y., Dong J., Shen X-Y.: Fabrication and characterization of poly(vinyl alcohol)/chitosan blend nanofibers produced by electrospinning method. Carbohydrate Polymers, **67**, 403–409 (2007). https://doi.org/10.1016/j.carbpol.2006.06.010

[15] Sun K., Li Z. H.: Preparations, properties and applications of chitosan based nanofibers fabricated by electrospinning. Express Polymer Letters, **5**, 342–361 (2011). https://doi.org/10.3144/expresspolymlett.2011.34

[16] Chen F., Liu P.: Conducting polyaniline nanoparticles and their dispersion for waterborne corrosion protection coatings. ACS Applied Materials and Interfaces, **3**, 2694–2702 (2011). https://doi.org/10.1021/am200488m

[17] Ekrem M., Avcı A.: Effects of polyvinyl alcohol nanofiber mats on the adhesion strength and fracture toughness of epoxy adhesive joints. Composites Part B: Engineering, **138**, 256–264 (2018). https://doi.org/10.1016/j.compositesb.2017.11.049

[18] Kakati N., Das G., Yoon Y. S.: Proton-conducting membrane based on epoxy resin-poly(vinyl alcohol)-sulfosuccinic acid blend and its nanocomposite with sulfonated multiwall carbon nanotubes for fuel-cell application. Journal of the Korean Physical Society, **68**, 311–316 (2016). https://doi.org/10.3938/jkps.68.311

[19] Tsou C-H., Zhao L., Gao C., Duan H., Lin X., Wen Y., Du J., Lin S-M., Suen M-C., Yu Y., Liu X., de Guzman M. R.: Characterization of network bonding created by intercalated functionalized graphene and polyvinyl alcohol in nanocomposite films for reinforced mechanical properties and barrier performance. Nanotechnology, **31**, 385703 (2020). https://doi.org/10.1088/1361-6528/ab9786

[20] Wang H., Qin X., Fei G., Tian M., Wen H., Zhu K.: Optimization of stability and properties of waterborne polyaniline-graft-poly(vinyl alcohol) nanocomposites with controllable epoxy content. Colloid and Polymer Science, **296**, 585–594 (2018). https://doi.org/10.1007/s00396-018-4283-1

[21] Yıldırım F., Ataberk N., Ekrem M.: Mechanical and thermal properties of a nanocomposite material which epoxy based and reinforced with polyvinyl alcohol nanofibers contained multiwalled carbon nanotube. Journal of Composite Materials, **55**, 1339–1347 (2020). https://doi.org/10.1177/0021998320969793

[22] Zahid M., Ali S., Saleem S., Salman M., Khan M.: Carbon nanoparticles/polyvinyl alcohol composites with enhanced optical, thermal, mechanical, and flame-retardant properties. Journal of Applied Polymer Science, **137**, e49261 (2020). https://doi.org/10.1002/app.49261

[23] Tamulevičius T., Peckus D., Tamulevičiene A., Vasiliauskas A., Čiegis A., Meškinis S., Tamulevičius S.: Dynamic optical properties of amorphous diamond-like carbon nanocomposite films doped with Cu and Ag nanoparticles. in 'Proceedings of SPIE 9163, Plasmonics: Metallic Nanostructures and Their Optical Properties XII, San Diego, California, USA' 91632J (2014). https://doi.org/10.1117/12.2061197

[24] Wong R. C. K., Schmitt D. R., Collis D., Gautam R.: Inherent transversely isotropic elastic parameters of overconsolidated shale measured by ultrasonic waves and their comparison with static and acoustic *in situ* log measurements. Journal of Geophysics and Engineering, **5**, 103–117 (2008). https://doi.org/10.1088/1742-2132/5/1/011

[25] Franco E., Meza J., Buiochi F.: Measurement of elastic properties of materials by the ultrasonic through-transmission technique. Dyna, **78**, 58–64 (2011).

[26] Honarvar F., Varvani-Farahani A.: A review of ultrasonic testing applications in additive manufacturing: Defect evaluation, material characterization, and process control. Ultrasonics, **108**, 106227 (2020). https://doi.org/10.1016/j.ultras.2020.106227

[27] Smirnova E., Sotnikov A., Shevelko M., Zaitseva N., Schmidt H.: Ultrasonic evidence of temperatures characteristic of relaxors in $PbFe_{2/3}W_{1/3}O_3$–$PbTiO_3$ solid solutions near the morphotropic phase boundary. Journal of Materials Science, **56**, 4753–4762 (2021). https://doi.org/10.1007/s10853-020-05613-3

[28] Zeighami M., Honarvar F.: New approaches for testing of adhesive joints by ultrasonic c-scan imaging technique. Materials Evaluation, **67**, 945–954 (2009).

[29] Bouhamed N., Souissi S., Marechal P., Amar M. B., Lenoir O., Leger R., Bergeret A.: Ultrasound evaluation of the mechanical properties as an investigation tool for the wood-polymer composites including olive wood flour. Mechanics of Materials, **148**, 103445 (2020). https://doi.org/10.1016/j.mechmat.2020.103445

[30] Oral I., Guzel H., Ahmetli G.: Determining the mechanical properties of epoxy resin (DGEBA) composites by ultrasonic velocity measurement. Journal of Applied Polymer Science, **127**, 1667–1675 (2013). https://doi.org/10.1002/app.37534

[31] Simonetti F., Cawley P., Demčenko A.: On the measurement of the Young's modulus of small samples by acoustic interferometry. Journal of the Acoustical Society of America, **118**, 832–840 (2005). https://doi.org/10.1121/1.1942387

[32] Castellano A., Foti P., Fraddosio A., Marzano S., Piccioni M.: A new ultrasonic immersion technique for the evaluation of damage induced anisotropy in composite materials. in '3rd International Balkans Conference on Challenges of Civil Engineering (3-BCCCE) Tirana, Albania', 273–282 (2016).

[33] El-Sabbagh A., Steuernagel L., Ziegmann G.: Characterisation of flax polypropylene composites using ultrasonic longitudinal sound wave technique. Composites Part B: Engineering, **45**, 1164–1172 (2013). https://doi.org/10.1016/j.compositesb.2012.06.010

[34] Ghodhbani N., Maréchal P., Duflo H.: Ultrasound monitoring of the cure kinetics of an epoxy resin: Identification, frequency and temperature dependence. Polymer Testing, **56**, 156–166 (2016). https://doi.org/10.1016/j.polymertesting.2016.10.009

[35] Lefebvre G., Wunenburger R., Valier-Brasier T.: Ultrasonic rheology of visco-elastic materials using shear and longitudinal waves. Applied Physics Letters, **112**, 241906 (2018). https://doi.org/10.1063/1.5029905

[36] Güzel H., Oral I., İşler H.: Measurement of the elastic properties of orthotropic materials by ultrasonic method. in 'Science and mathematics research papers' (eds.: Öztekin A., Mansuroglu N.) Gece Publishing, Ankara, 57–87 (2019).

[37] Mistou S., Karama M.: Determination of the elastic properties of composite materials by tensile testing and ultrasound measurement. Journal of Composite Materials, **34**, 1696–1709 (2000). https://doi.org/10.1106/uy4r-fg3h-hkgw-ud3q

[38] Rajzer I., Rom M., Blazewicz M.: Production of carbon fibers modified with ceramic powders for medical applications. Fibers and Polymers, **11**, 615–624 (2010). https://doi.org/10.1007/s12221-010-0615-8

[39] Piekarczyk W., Kata D.: Methodology for determining material constants of anisotropic materials belonging to the transversely isotropic system by ultrasound method. Ultrasonics, **71**, 199–204 (2016). https://doi.org/10.1016/j.ultras.2016.06.015

[40] Rajzer I., Grzybowska-Pietras J., Janicki J.: Fabrication of bioactive carbon nonwovens for bone tissue regeneration. Fibres and Textiles in Eastern Europe, **84**, 66–72 (2011).

[41] Song I., Suh M., Woo Y-K., Hao T.: Determination of the elastic modulus set of foliated rocks from ultrasonic velocity measurements. Engineering Geology, **72**, 293–308 (2004). https://doi.org/10.1016/j.enggeo.2003.10.003

[42] Dahmen S., Ketata H., Ben Ghozlen M. H., Hosten B.: Elastic constants measurement of anisotropic olivier wood plates using air-coupled transducers generated lamb wave and ultrasonic bulk wave. Ultrasonics, **50**, 502–507 (2010). https://doi.org/10.1016/j.ultras.2009.10.014

[43] Lasaygues P., Pithioux M.: Ultrasonic characterization of orthotropic elastic bovine bones. Ultrasonics, **39**, 567–573 (2002). https://doi.org/10.1016/S0041-624X(02)00261-5

[44] Papadakis E. P.: Ultrasonic phase velocity by the pulse-echo-overlap method ıncorporating diffraction phase corrections. Journal of the Acoustical Society of America, **42**, 1045–1051 (1967). https://doi.org/10.1121/1.1910688

[45] Vary A.: Ultrasonic measurement of material properties. Research Techniques in Nondestructive Testing, **4**, 306–356 (1980).

[46] Charles J. H.: Handbook of nondestructive evaluation. McGraw-Hill Education, New York (2013).

[47] Gold L.: Compilation of body wave velocity data for cubic and hexagonal metals. Journal of Applied Physics, **21**, 541–546 (1950). https://doi.org/10.1063/1.1699703

[48] Musgrave M. J. P.: On the propagation of elastic waves in aeolotropic media I. General principles. Proceedings of the Royal Society A: Mathematical, Physical and Engineering Sciences, **226**, 339–355 (1954). https://doi.org/10.1098/rspa.1954.0258

[49] Lee M. W.: Velocity ratio and its application to predicting velocities. U.S. Geological Survey Bulletin, **2197**, 1–15 (2003).

[50] Pickett G. R.: Acoustic character logs and their applications in formation evaluation. Journal of Petroleum Technology, **15**, 659–667 (1963). https://doi.org/10.2118/452-pa

[51] Nanekar P., Shah B.: Characterization of material properties by ultrasonic. BARC Newsl, **249**, 25–38 (2003).

[52] Perepechko I. I.: Acoustic methods of investigating polymers. Mir, Moscow (1975).

[53] Akankpo O., Essien U.: Determination of Lame's constants of surface soils and shallow sediments from seismic wave velocities. International Journal of Scientific und Engineering Research, **6**, 1052–1065 (2015).

[54] Popa M., Arnautu M., Davydov Y.: The interface in polymer matrix composites. in 'Handbook of poymer blends and composites' (eds.: Kulshreshtha A. K., Vasile C.) Rapra, London, 251–298 (2002).

[55] de Oliveira F. G. R., Sales A.: Relationship between density and ultrasonic velocity in brazilian tropical woods. Bioresource Technology, **97**, 2443–2446 (2006). https://doi.org/10.1016/j.biortech.2005.04.050

[56] Oral I., Ahmetli G.: Ultrasonic characterisation of epoxy resin/polyethylene terephthalate (PET) char powder composites. Medžıagotyra, **22**, 553–559 (2016). https://doi.org/10.5755/j01.ms.22.4.12190

[57] Ilic J.: Dynamic moe of 55 species using small wood beams. Holz als Roh- und Werkstoff, **61**, 167–172 (2003). https://doi.org/10.1007/s00107-003-0367-8

[58] Oral I.: Ultrasonic characterization of conductive epoxy resin/polyaniline composites. Journal of Applied Polymer Science, **132**, 42748 (2015). https://doi.org/10.1002/app.42748

[59] Odetoye T. E., Ashaolu O. O.: Preparation and water absorption properties of parinari polyandra fruit shell reinforced epoxy composites. FUOYE Journal of Engineering and Technology, **5**, 175–178 (2020). https://doi.org/10.46792/fuoyejet.v5i2.532

[60] El-Hadi Z. A., Khalida F. A., El-Kheshen A. A., Moustaffa F. A.: Density and molar volume of some high lead silicate glasses. Communications Faculty of Sciences University of Ankara Series B Chemistry and Chemical Engineering, **41**, 33–50 (1995). https://doi.org/10.1501/Commub_0000000402

[61] Ekrem M.: Mechanical properties of MWCNT reinforced polyvinyl alcohol nanofiber mats by electrospinnig method. El-Cezerî Journal of Science and Engineering, **4**, 190–200 (2017). https://doi.org/10.31202/ecjse.305851

[62] Afifi H. A.: Ultrasonic pulse echo studies of the physical properties of PMMA, PS, and PVC. Polymer – Plastics Technology and Engineering, **42**, 193–205 (2003). https://doi.org/10.1081/PPT-120017922

[63] Gercek H.: Poisson's ratio values for rocks. International Journal of Rock Mechanics and Mining Sciences, **44**, 1–13 (2007). https://doi.org/10.1016/j.ijrmms.2006.04.011

[64] Kaye G. W. C., Laby T. H.: Tables of physical and chemical constants. Zeitsc Zeitschrift für Kristallographie – Crystalline Materials, 212, 400 (1997). https://doi.org/10.1524/zkri.1997.212.5.400

[65] Oral I., Guzel H., Ahmetli G., Gur C. H.: Determining the elastic properties of modified polystyrenes by sound velocity measurements. Journal of Applied Polymer Science, **121**, 3425–3432 (2011). https://doi.org/10.1002/app.33860

[66] Oral I., Guzel H., Ahmetli G.: Ultrasonic properties of polystyrene-based composites. Journal of Applied Polymer Science, **125**, 1226–1237 (2012). https://doi.org/10.1002/app.34926

[67] Graham J., Houlsby G. T.: Anisotropic elasticity of a natural clay. Géotechnique, **33**, 165–180 (1983). https://doi.org/10.1680/geot.1983.33.2.165

[68] Jovičić V., Coop M. R.: The measurement of stiffness anisotropy in clays with bender element tests in the triaxial apparatus. Geotechnical Testing Journal, **21**, 3–10 (1998).

[69] Lings M. L.: Drained and undrained anisotropic elastic stiffness parameters. Géotechnique, **51**, 555–565 (2001). https://doi.org/10.1680/geot.2001.51.6.555